



HAL
open science

Modeling and simulation of drying operation in PVC powder production line: a pneumatic dryer model

Antoine Aubin, Renaud Ansart, Mehrdji Hemati, Thierry Lasuye, Marc Branly

► To cite this version:

Antoine Aubin, Renaud Ansart, Mehrdji Hemati, Thierry Lasuye, Marc Branly. Modeling and simulation of drying operation in PVC powder production line: a pneumatic dryer model. 18th Symposium in the biennial series of International Drying Symposia Series (IDS2012), Nov 2012, Xiamen, China. pp.0. hal-04023549

HAL Id: hal-04023549

<https://hal.science/hal-04023549>

Submitted on 10 Mar 2023

HAL is a multi-disciplinary open access archive for the deposit and dissemination of scientific research documents, whether they are published or not. The documents may come from teaching and research institutions in France or abroad, or from public or private research centers.

L'archive ouverte pluridisciplinaire **HAL**, est destinée au dépôt et à la diffusion de documents scientifiques de niveau recherche, publiés ou non, émanant des établissements d'enseignement et de recherche français ou étrangers, des laboratoires publics ou privés.



Open Archive Toulouse Archive Ouverte (OATAO)

OATAO is an open access repository that collects the work of Toulouse researchers and makes it freely available over the web where possible.

This is an author-deposited version published in: <http://oatao.univ-toulouse.fr/>
Eprints ID: 8364

Official URL: <http://innova-xiamen.com/IDS2012.html>

To cite this version:

Aubin, Antoine and Ansart, Renaud and Hemati, Mehdi and Lasuye, Thierry and Branly, Marc *Modeling and simulation of drying operation in PVC powder production line: a pneumatic dryer model*. In: 18th Symposium in the biennial series of International Drying Symposia Series (IDS2012), 11-15 Nov 2012, Xiamen, China.

Any correspondence concerning this service should be sent to the repository administrator:
staff-oatao@inp-toulouse.fr

MODELING AND SIMULATION OF DRYING OPERATION IN PVC POWDER PRODUCTION LINE: A PNEUMATIC DRYER MODEL.

A. Aubin^{1,2}, R. Ansart^{1,2}, M. Hemati^{1,2}, T. Lasuye³, M. Branly³

¹*Université de Toulouse ; INPT, UPS ; Laboratoire de Génie Chimique ; 4, Allée Emile
Monso, F-31030 Toulouse, France
Tel.: +33 5 34 32 36 93, E-mail: antoine.aubin@ensiacet.fr*

²*CNRS ; Laboratoire de Génie Chimique ; F-31030 Toulouse, France*

³*INEOS - Société Artésienne de Vinyle,
Chemin des soldats 62670 Mazingarbe, France
Tel.: +33 3 21 72 83 17, E-mail: Thierry.lasuye@ineos.com*

Abstract: A one-dimensional steady-state model is developed to simulate drying of PVC powder in a pneumatic dryer. In this model, a two-phase continuum model was used to describe the steady-state flow of a dilute dispersed phase (wet PVC powder) and a continuous phase (humid air) through dryer. The particle scale kinetics was obtained by immersion of a fixed mass of wet PVC's particles (cake) in a batch dense fluidized bed containing inert hot particles (glass bead). The drying kinetics was described by a shrinking core type model and integrated in pneumatic dryer model. The results show that the inlet temperature is the most important parameter in the operation. The drying rate is controlled by a two-stage process. The first stage corresponds to the surface water evaporation, and the second to the pore water evaporation.

Keywords: pneumatic dryer, PVC, shrinking core, kinetic, model

INTRODUCTION

In PVC powder production line, after the polymerization step, a suspension, composed of water and PVC particles, is obtained. Most of this suspension's water is eliminated during a centrifugation step, leading to a wet porous powder, called "cake". The cake drying occurs essentially in a pneumatic dryer coupled with a fluidized bed dryer that role is to eliminate the residual humidity of PVC (less than 0,05 kg water/kg dry PVC). This operation consumes a lot of energy, between 125 and 375 J / kg dry PVC, in accordance to the operating conditions and the PVC's grade.

The pneumatic dryer is a technology commonly used in order to eliminate free or barely-bound water. A pneumatic dryer is a continuous, convective dryer with dilute solid transport. This technology presents numerous advantages (Strumillo 1986, Ouyang et al., 2003) such as:

- the short resident time of particles allows to dry thermosensible product,
- in parallel flow, high temperature can be applied at the inlet giving high thermal efficiency,
- the dryer can be used as a transport system.

With the purpose to optimize the drying process, i.e. reduces the energy consumption, this study focuses on:

- (i) the acquisition of the kinetics data in a batch dense fluidized bed,
- (ii) the modeling of the dehydration of PVC's particles in a pneumatic dryer.

DRYING KINETICS

Porous media drying is a complex problem, still not well-understand despite of the numerous studies that can be found in the literature, due to the coupled exchanges (mass, heat, and momentum transfers) between the gas and the particles (Kowalski, 2007, Prat, 2002, Segura and Toledo, 2005).

As shown in figure 1, during the drying of a porous particle, two periods can be distinguished. The first period consists in the elimination of the free water located at its surface. In this case the evaporation is controlled by external transfers depending on the local relative velocity between the air and the particles, called slip velocity. These transfers depending on the drying technology have been widely studied, and the literature provides a lot of correlations, some times contradictory, for its estimation. In the second period, the water located in the particle's pore, is eliminated: the drying is

controlled by a combination between internal and external transfers.

In the case of porous particle, according to the nature of the solid, the internal transfers can be driven by one or a combination of several elementary mechanisms such as:

- the capillarity effect,
- the migration in adsorbed phase (or liquid diffusion),
- the vapor diffusion through the pores.

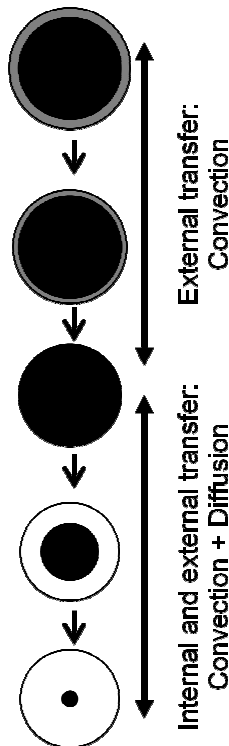


Fig. 1: Particle drying

PVC PROPERTIES

The SEM pictures of PVC particles, produced by the suspension polymerization process, show that each particle can be represented by a “Pellet-grain” structure constituted of elementary grains of 1 μm diameter (see Fig. 2). The pore size distribution, obtained by mercury porosimetry, shows two families of pores (see Fig. 3):

- From 200 to 10 000 nm: the space between the primary particles.
- From 50 to 200 nm: the primary particles’ porosity.

According to the Kelvin’s law, the effect of the pore mean size diameter on water activity can be neglected for the values greater than 10 nm. According to the figure 3, the capillary effects can be neglected in the case of PVC’s particle drying.

In the aim of characterizing the affinity of PVC toward the water vapor, some experiments

concerning the sorption equilibrium have been carried out. The results show that the PVC has a small affinity with water vapor (e.g. in an atmosphere containing 75% of relative humidity, the PVC’s equilibrium humidity is about 2.4 g of water / kg of PVC). Moreover the PVC is insoluble in water, so the migration in adsorbed phase can be neglected.

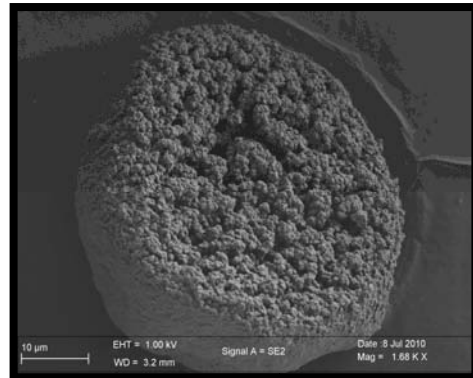


Fig 2: SEM picture of a PVC particle

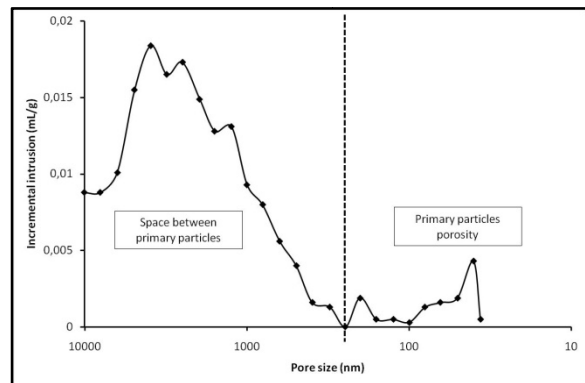


Fig. 3: pores size distribution of PVC’s particle

According to the nature of PVC’s particles, the only elementary mechanism can be controlled the internal transfer is the water vapor’s diffusion through the pores.

In order to minimize the external effects, the kinetics study was performed by immersion of a fixed mass of wet PVC’s particles (cake) in a batch dense fluidized bed containing inert hot particles (glass bead). The complete description of the apparatus and that of the experimental procedure are presented elsewhere (Aubin et al; 2012t). The influence of the temperature, the water vapor pressure, the PVC grades and the fluidizing gas velocity are investigated. The evolution of the PVC humidity versus time is described correctly by a “shrinking core” type model.

KINETICS MODEL AT PARTICLE SCALE

In the shrinking core type model, as shown in figure 4, particle’s humidity is concentrated in a moist core which will shrink during the drying and so form a dry crust at particle’s surface (Mezhericher et al.; 2008; Cheong et al., 1986).

The evaporation takes place at the surface of the moist core, and the water vapor diffuses through the dry crust. To determine the drying kinetics the mass balance on a single particle is realized. The balance takes into account the water vapor diffusion through the crust and water vapor exchange at particle's surface. So, the rate of mass transfer can be expressed as:

$$\dot{N}_w = K_y \cdot (Y^* - Y^\infty). \quad (1)$$

Where Y^* is the equilibrium humidity, Y^∞ the humidity of the air far from the particle, and K_y is the global mass transfer coefficient expressed as:

$$K_y = \frac{k_y}{Bi_M \cdot (d_p/d_h)^{-1} + 1}. \quad (2)$$

Where k_y is the convective mass transfer coefficient, d_p and d_h the respective diameter of the particle and the humid core, and Bi_M the dimensionless number called Biot number relative to mass transfer. This number represents the competition between external and internal transfer:

$$Bi_M = \frac{k_y \cdot R}{D_{app} \cdot \rho_g}. \quad (3)$$

Where R is the particle's radius, ρ_g the gas density, and D_{app} the diffusion coefficient of water vapor in the air within a pore, calculated from the binary diffusion coefficient, D_{bin} :

$$D_{app} = D_{bin} \frac{\chi}{\tau} \quad (4)$$

The porosity, χ , and the tortuosity, τ , values are indicated in the table 3.

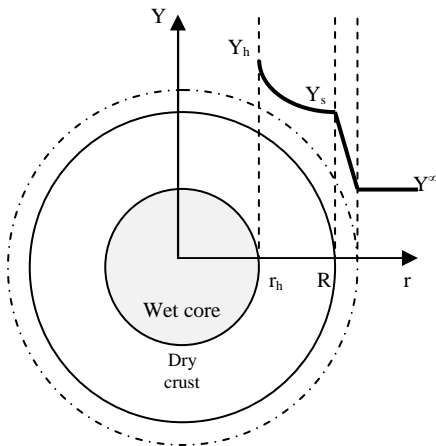


Fig. 4: The shrinking core model

This model has been validated in a previous study of the drying kinetics at particle's scale obtained in fluidized bed (Aubin et al.; 2012). The results have shown that the resistance of internal transfers is about 1.5 times bigger than the external resistance ($Bi_M \cong$

1.5). This shows the strong effect of external exchanges on the drying kinetic.

ONE DIMENSION PNEUMATIC DRYER MODEL

Table 1: Main equations

Mass balances	
Solid phase	$\frac{d}{dz} (\alpha_p \cdot \rho_p \cdot U_p) = \Gamma_p$ (5)
Gas phase	$\frac{d}{dz} (\alpha_g \cdot \rho_g \cdot U_g) = \Gamma_g = -\Gamma_p$ (6)
Energy Balances	
Solid phase	$F_p^0 \cdot \frac{dH_p}{dz} = Q_{g \rightarrow p} + A_c \cdot \Gamma_p \cdot H_w^g$ (7)
Gas phase	$F_g^0 \cdot \frac{dH_g}{dz} = Q_{p \rightarrow g} + Q_{w \rightarrow g} + A_c \cdot \Gamma_g \cdot H_w^g$ (8)
Momentum balances	
Solid phase	$\frac{\partial}{\partial z} (\alpha_p \cdot \rho_p \cdot U_p^2) = \alpha_p \cdot \frac{\partial P}{\partial z} - \alpha_p \cdot \rho_p \cdot g + I_{g \rightarrow p}$ (9)
Gas phase	$\frac{\partial}{\partial z} (\alpha_g \cdot \rho_g \cdot U_g^2) = \alpha_g \cdot \frac{\partial P}{\partial z} - \alpha_g \cdot \rho_g \cdot g + I_{p \rightarrow g} + [U_p - U_g] \cdot \Gamma_g + F_{f, w \rightarrow g}$ (10)
Humidity transport equations	
Solid phase	$\frac{dX}{dz} = \frac{A_c \cdot \Gamma_p}{F_p^0}$ (11)
Gas phase	$\frac{dY}{dz} = \frac{A_c \cdot \Gamma_g}{F_g^0} = -\frac{F_p^0}{F_g^0} \cdot \frac{dX}{dz}$ (12)

Model's hypothesis

The aim of this study is to model a pneumatic dryer using the particle scale kinetics previously elaborated. In this model, a two-phase continuum model was used to describe the steady-state flow of a diluted dispersed phase (wet powder) and a continuous phase through a pneumatic dryer. The model is based on the following assumptions:

- Mass, energy and momentum balances occur between the two phases.
- The frictions forces between the dispersed phase and the wall can be neglected.
- The continuous phase, composed by a mixture of water vapor and other gas, is considered as an ideal phase.
- The particles are spherical and composed of a homogeneous porous matrix.
- The particles size's distribution is considered as monodisperse
- Liquid water and PVC density are constant.

- Electrostatic forces and surface tension effects are neglected.
- The wall heat loss is neglected.

Balance equations

The mass, energy, and momentum balances developed in one-dimensional steady-state for both phases are presented in table 1. The transport equations for solid and gas humidity, deduced from the mass balances, are also included in this table.

Complementary equations

The volume rate of mass transfer Γ_p , is expressed from the rate of mass-transfer \dot{N}_w .

$$\Gamma_p = -\Gamma_g = -\alpha_p \cdot s_p \cdot \dot{N}_w. \quad (13)$$

Where α_p is the local volume fraction of solid and s_p the specific surface area of a particle.

As shown on figure 1, the particle's drying occurs in two periods (Levy, 1998). During the first period, the mass transfer is convective. Then the expression of the global mass transfer coefficient can be simplified as following:

$$K_y = k_y \cdot \left(\frac{\rho_p \cdot X}{\rho_{water}} + 1 - \chi \right). \quad (14)$$

Where ρ_p is the solid density, ρ_{water} the liquid water density and χ the particle porosity.

During the second period, the mass transfer is convective and diffusive, and the global mass transfer is given by equation (2). This period starts when the surface humidity is totally eliminated, which means that the particle's humidity reaches a critical humidity, X_c :

$$X_c = \frac{\rho_{water} \cdot X}{\rho_p}. \quad (15)$$

The energy transfer between the two phases is expressed as followed:

$$Q_{g \rightarrow p} = -Q_{p \rightarrow g} = \alpha_p \cdot A_c \cdot s_p \cdot h \cdot (T_g - T_p). \quad (16)$$

Where A_c is the pipe cross section, h the heat-transfer coefficient, and T_p and T_g , the, respectively, solid and gas phase temperature.

Only the forces due to dragging are taken into account in the momentum transfer:

$$I_{g \rightarrow p} = -I_{p \rightarrow g} = \frac{3 \cdot \alpha_p \cdot \rho_g \cdot U_r^2 \cdot C_d}{4 \cdot d_p}. \quad (17)$$

Where U_r is the slip velocity.

The drag coefficient, C_d , is calculated by the Wen et Yu correlation (Schiller and Naumann, 1935):

$$C_d = \frac{24}{Re} (1 + 0.15 Re^{0.687}) \alpha_g^{-1.7} \quad (18)$$

The friction force between the pipe and the continuous phase is estimated by:

$$F_{f,w \rightarrow g} = \frac{f \cdot \rho_g}{2 \cdot D_{pipe}} \cdot U_g^2 \quad (19)$$

The friction factor, f , is calculated by the Blasius formula:

$$f = \frac{64}{Re_{pipe}} \text{ if } Re_{pipe} < 2100 \quad (20)$$

$$f = \frac{0.0791}{Re_{pipe}^{1/4}} \text{ if } Re_{pipe} > 10000 \quad (21)$$

Transfer coefficients

Some empirical correlations can be used to calculate the heat-transfer coefficient from the Nusselt number, Nu , as a function of the Reynolds, Re , and Prandtl, Pr , numbers. Their expressions are resumed in table 2.

The Chilton and Colburn analogy is used in order to calculate the mass transfer coefficient:

$$\frac{Sh}{Re \cdot Sc^{1/3}} = \frac{Nu}{Re \cdot Pr^{1/3}} \quad (22)$$

As the gas phase is only composed of air and steam, the Prandtl number can be considered equal to the Schmidt number, Sc . So the mass-transfer coefficient can be calculated from the correlations presented in the table 2 by substituting the Nusselt number by the Sherwood number, Sh , and the Prandtl number by the Schmidt number.

Table 2: Empirical correlations from literature

Ranz-Marshall (Levi-Hevroni et al., 1995)	$Nu = 2 + 0.6 \cdot Re^{0.5} Pr^{0.333}$ (23)
Baeyens et al. (1995)	$Nu = 0.15 Re$ (24)
De Brandt (Baeyens et al., 1995)	$Nu = 0.16 Re^{1.3} Pr^{0.67}$ (25)
Gamson (Kerker and Terwiesch, 1985)	$Nu = 1.06 Re^{0.59} Pr^{0.33}$ (26)
Khotari (Kunii and Levenspiel, 1969)	$Nu = 0.003 Re^{1.3}$ (27)
Bandrowski (1977)	$Nu = 0.00114 \alpha_p^{-0.5984} Re^{0.8159}$ (28)

Most of the correlations have been developed for a single particle, but in pneumatic dryers, collisions between particles occur. This has an important influence on the boundary layer surrounding the particle surface, and so on the transfers' rate. In order to model this phenomenon, Bandrowski (1977) expressed the Nusselt number as a function of the solid volume fraction, α_p .

RESULTS AND DISCUSSION

The simulation data are resumed in table 3. The figures 5 and 6 represent the theoretical results obtained using the different correlations gathered in table 2 and the experimental founding of Baeyens et al. (1995). The results obtained with correlations of Ranz-Marshall (developed for a single particle), Gamson, and Kothari (developed for a fluidized bed) show important deviations with experimental results and so are not presented on these figures.

Table 3: Simulation data

Data	Baeyens et al (1995)
Mean particles diameter (μm)	180
Solids density ($\text{kg}\cdot\text{m}^{-3}$)	1116
Porosity (-)	0,15
Tortuosity (-)	8
Pipe diameter (m)	1.25
Pipe length (m)	25
Inlet PVC humidity (kg water / kg dry PVC)	0.26
Critical PVC humidity (kg water / kg dry PVC)	0.134
Inlet air temperature ($^{\circ}\text{C}$)	127
Dry air mass flowrate ($\text{kg}\cdot\text{h}^{-1}$)	46480
Dry solid mass flowrate ($\text{kg}\cdot\text{h}^{-1}$)	6670

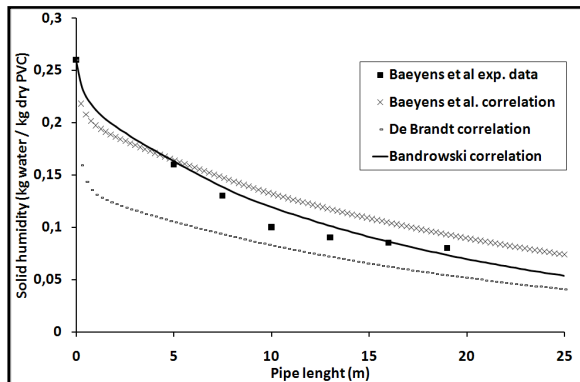


Fig. 5: Comparison between experimental data and simulation results with different correlations: evolution of particle's humidity

The differences observed between experimental data and theoretical results can be explained by the worst dispersion of the wet cohesive PVC in the gas phase at the pipe's inlet zone. The theoretical results which fit the best the experimental data have been obtained using Bandrowski's correlation. This can be

explained by the effect of the slip velocity on the Reynolds number, and so on the heat and mass transfer coefficients. As shown on Figure 7, this magnitude is really important at the inlet and progressively decreases along the dryer. This leads to very important variation of the transfer coefficients (see Fig. 8). In Bandrowski correlation, this effect is attenuated by the solid volume fraction of the dispersed phase. Indeed, as the solid go through the dryer, it is dispersed by the gas phase and its volume fraction decreases strongly at the dryer's inlet.

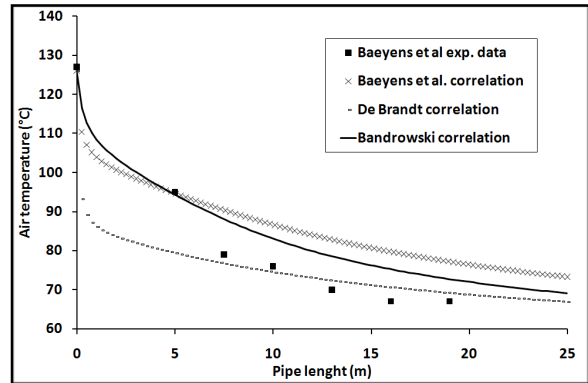


Fig. 6: Comparison between experimental data and simulation results with different correlations: evolution of air temperature

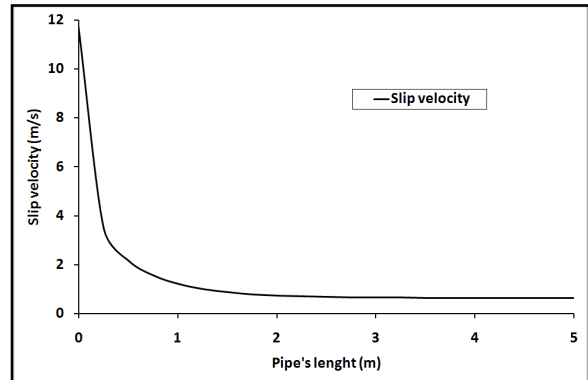


Fig. 7: Evolution of slip velocity along the dryer

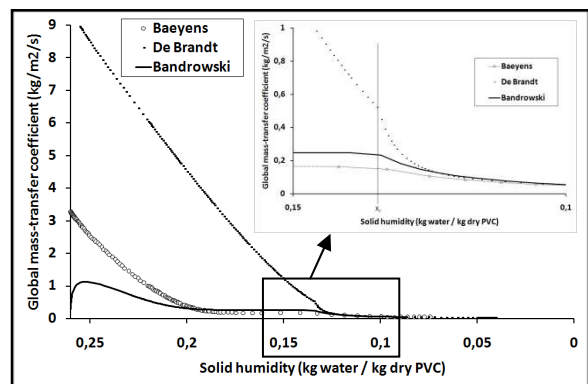


Fig. 8: Evolution of the global mass-transfer coefficient with the solid humidity

These results show that a major part of the transfers occurs in the acceleration zone (the pipe's first meter

where the solid velocity increases). Particle temperature increases until a constant value, which corresponds to the constant rate drying period. Due to the evaporation surface reduction, a small rise can be observed. When particle humidity reaches the critical humidity, the falling rate drying period starts, and as the drying rate decreases, the particle temperature increase will be stronger (figure 9).

Parameters study

The results of the following simulations have been obtained using the Bandrowski's correlation (see table 3).

The effect of dry air mass flowrate has been examined between 25 and 46.4 t/h. As shown on figure 9, this parameter has a small influence on the drying rate above 35 t/h. The air velocity influences the drying rate only in the acceleration zone, then the slip velocity is equal to the terminal settling velocity. At the dryer's outlet the air is far to be saturated, so the decrease of the dry air flowrate does not affect the drying driving force significantly (e.g. a decrease of dry air flowrate from 46 t/h to 35 t/h increases the outlet solid humidity from 0.054 to 0.067 kg water / kg dry PVC, and a decrease of dry air flowrate from 35 t/h to 25 t/h increases the outlet solid humidity from 0.067 to 0.097 kg water / kg dry PVC).

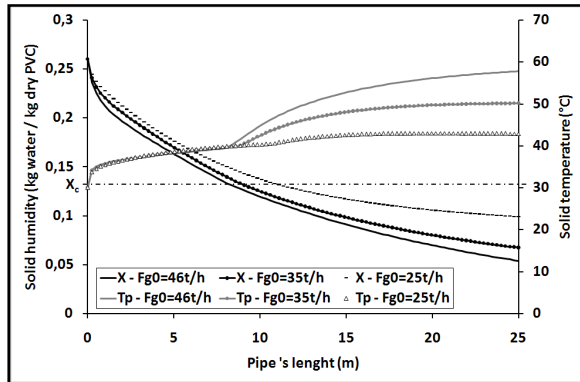


Fig. 9: Evolution of solid humidity and temperature along the riser for different dry air flowrates: 46.4 t/h, 35 t/h, and 25 t/h.

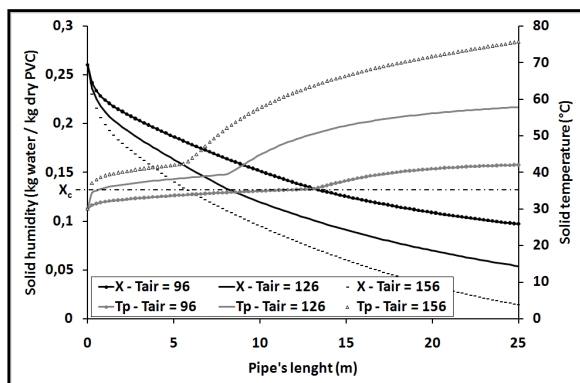


Fig. 10: Evolution of solid humidity and temperature along the riser for different inlet air temperatures: 126°C, 96°C, and 156°C.

Concerning the inlet air temperature, the figure 10 shows a dominant effect (e.g. an increase of inlet air temperature from 96°C to 156°C decreases the outlet solid humidity from 0.097 to 0.014 kg water / kg dry PVC). Indeed, increasing the temperature lead to a more important heat-transfer driving force. But as the equilibrium humidity depends on the temperature, it will also increase the mass-transfer driving force.

The inlet air humidity effect has been investigated between 0 and 0.0105 kg water / kg dry air. The last value corresponds to an atmospheric air (15°C) almost saturated (98.4% of relative humidity). As shown on figure 11, such an increase of inlet air humidity increases the outlet solid humidity from 0.052 to 0.054 kg water / kg dry PVC. This increase shows that the inlet air humidity, which is a sustained parameter, slightly influences the drying driving force.

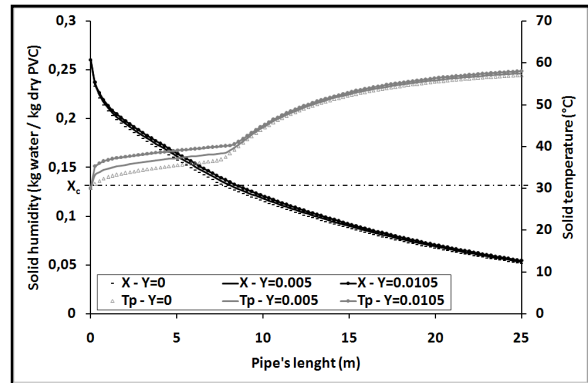


Fig. 11: Evolution of solid humidity and temperature along the riser for different inlet air humidity: 0 ; 0.005 ; 0.0105 kg water / kg dry air

It can be noticed that the solid temperature is influenced by:

- the dry air flowrate during the falling drying rate period only,
- the air humidity during the constant drying rate period only,
- the air temperature influences it during both periods.

In fact the temperature stage value of the constant drying period is controlled by the drying driving forces. As shown in equations (1) and (13), this force depends only on the air humidity, Y^∞ , and the equilibrium humidity, Y^* , which is directly related to the solid temperature. In the falling drying rate period, the solid temperature increases until the thermal equilibrium with the air, which is controlled by the dry air flowrate and temperature.

CONCLUSIONS

A one-dimensional steady-state model for pneumatic dryer was established. This model is applied for the drying process of wet PVC powder. The drying rate is controlled by convective transfer in the first period and by convective and diffusive transfer in the second. The first period corresponds to

the surface water drying; besides the second corresponds to the evaporation of the water in the pores, simulate by a shrinking core model. The model takes into account the convective heat, masse and momentum transfers. Parameters study shows that the inlet temperature is the most important parameter in the operation. But this model does not take into account the wet powder dispersion, which is certainly the limiting step of this process.

NOMENCLATURE

Ac	pipe cross section	m ²
C _d	drag coefficient	-
C _{p_g}	specific heat of the gas	J.kg ⁻¹ K ⁻¹
d _p	particle's diameter	m
d _h	wet core's diameter	m
D _{pipe}	pipe diameter	m
D _{bin}	diffusion coefficient of water vapor	m ² .s ⁻¹
D _{app}	diffusion coefficient in the pores	m ² .s ⁻¹
f	friction factor	-
F _f	friction force	kg.m ⁻² .s ⁻²
F _k ^o	dry mass flowrate of the k-phase	kg.s ⁻¹
g	acceleration due to gravity	m.s ⁻²
h	heat-transfer coefficient	W.m ⁻² K ⁻¹
h _{wall}	wall heat-transfer coefficient	W.m ⁻² K ⁻¹
H _k	mass enthalpy of the k phase	J.kg ⁻¹
H _w ^g	water vapour mass enthalpy	J.kg ⁻¹
I _{q→k}	interphase force from q to k phase	kg.m ⁻² .s ⁻²
k _y	convective mass-transfer coefficient	kg.m ⁻² .s ⁻¹
K _y	global mass-transfer coefficient	kg.m ⁻² .s ⁻¹
N _w	rate of mass transfer	kg.m ⁻² .s ⁻¹
P	gas ambient pressure	Pa
Q _{q→k}	heat transfer from q to k phase	W.m ⁻¹
s _p	specific surface area	m ² .m ⁻³
T	temperature	K
U _k	average velocity of the k-phase	m.s ⁻¹
U _r	relative or slip velocity	m.s ⁻¹
X	solid humidity	kg.kg _{dry} ⁻¹
X _c	critical humidity	kg.kg _{dry} ⁻¹
Y	air absolute humidity	kg.kg _{dry} ⁻¹
Y*	interface air/water humidity	kg.kg _{dry} ⁻¹
z	pipe's height	m

Greek letters

α _k	volume fraction of the k-phase	-
ρ _k	density of the k-phase	kg.m ⁻³
λ _g	thermal conductivity of the gas	W.m ⁻¹ K ⁻¹
μ _g	viscosity of the gas	Pa.s
Γ _k	volume rate of mass-transfer	kg.m ⁻³ .s ⁻¹
χ	particle's porosity	-
τ	pore's tortuosity	-

Subscripts

g	gas
p	particle
w	wall

Dimensionless numbers

Nu	Nusselt number	$Nu = \frac{h.d_p}{\lambda_g}$
Pr	Prandtl number	$Pr = \frac{Cp_g.\mu_g}{\lambda_g}$
Re	Particle Reynolds number	$Re = \frac{\rho_g.U_r.d_p}{\mu_g}$
Re _{pipe}	Pipe Reynolds number	$Re_{pipe} = \frac{\rho_g.U_g.D_{pipe}}{\mu_g}$
Sc	Schmidt number	$Sc = \frac{\mu_g}{\rho_g.D_{bin}}$
Sh	Sherwood number	$Sh = \frac{k_y.d_p}{D_{bin}}$

REFERENCES

- Aubin A., Hemati M., Lasuye T., and Branly M. (2012), Model and simulation of drying operation in PVC powder production line: Experimental and theoretical study of drying kinetics on particle scale, 7ème colloque Sciences et Technologie des Poudres, Toulouse, France, July 4-7, 2012.
- Baeyens J., van Gauwbergen D., and Vinckier I. (1995), Pneumatic drying: the use of a large-scale experimental data in a design procedure, Powder Technology, Vol. 83, pp. 139-148.
- Bandrowdki J., and Kaczmarzyk G. (1977), Gas-to-particle heat transfer in vertical pneumatic conveying of granular materials, Chemical Engineering Science, Vol. 33, pp. 1303-1310.
- Cheong H. W., Jeffreys G. V., and Mumford C. J. (1986), A receding interface model for the drying of slurry droplets, AIChE Journal, Vol. 32, pp. 1334-1346
- Kerker L., and Terwiesch B. (1985), Kunststoff-Handbuch PVC, Backer and Brown.
- Kowalski S. J. (2007), Drying of porous materials, Springer.
- Kunii D., Levenspiel O. (1969), Fluidization Engineering, Wiley, New York.
- Levi-Hevroni D., Levy A., and Borde I. (1995), Mathematical modeling of drying of liquid/solid slurries in steady state one dimensional flow, Drying Technology, Vol. 13, pp. 1187-1201.
- Levy A., and Borde I. (1998), Steady state one dimensional flow model for a pneumatic dryer, Chemical Engineering and Processing, Vol. 38, pp.121-130
- Mezhericher M., Levy A., and Borde I. (2008), Heat and mass transfer of single droplet/wet particle drying, Chemical Engineering Science, Vol. 63, pp. 12-23
- Ouyang S., Mao S. M., Rhodes M., and Potter O. E. (2003), Short contact time gas-solid systems, Reviews in chemical engineering, Vol. 19, No. 2, pp. 133-228.

Prat M., (2002), Recent advances in pore-scale model for drying of porous media, Chemical Engineering Journal, Vol. 86, pp. 153-164.

Schiller L., and Naumann Z. (1935), Ver. Deutsch Ing., Vol. 77, pp 318.

Segura L.A., and Toledo P.G. (2005), Pore-level modeling of isothermal drying of pore networks. Effect of gravity and pore shape and size distributions on saturation and transport parameters, Chemical Engineering Journal, Vol. 111, pp. 237-252.

Strumillo, C and Kudra, T. (1986), Drying: principles, applications and design, Gordon and Breach Science Publishers, New York.